

A COMBINED ENERGY DISSIPATION DEVICE AND ITS APPLICATION ON A WEAK-STORY

Fatih Sutcu¹, Norio Inoue², Norio Hori³

¹Research Associate PhD, Istanbul Technical University

²Professor, Tohoku University-Japan

³Research Associate, Tohoku University-Japan

ABSTRACT

A weak-story in a multi-story building may cause excessive displacement during a severe ground motion. To prevent this effect, this study proposes an energy dissipation device combined of viscous dampers and displacement controlling limiter. The limiter which has a hardening type force-displacement relationship compensates the low capacity of the structure on the weak-story and provides a uniform ductility distribution among the stories. Considering the mentioned merit of limiter device, an energy-based damper design method was developed to obtain the necessary amount of damper. Technically speaking, damper design requires predicting the structural response accurately, which leads to iterative dynamic response analysis and sophisticated time history analysis. Proposed energy-based method does not require time history analysis as it assumes uniform ductility distribution, which can be obtained by the limiter.

KEYWORDS: Energy based design, earthquake resistant design, viscous damper, displacement control

1. INTRODUCTION

Viscous-dampers are well known to reduce the displacements of a structure subjected to an earthquake [Hanson R.D. *et al.* 1993]. However a weak-story in a multi-story building will cause excessive displacement, which causes a non-uniform displacement distribution among the stories. To prevent this effect, a combined energy dissipation device is proposed in this study. The combined device which was originally developed by Kawamata [Kang J. *et al.* 2004], absorbs energy and decreases the structural response during a moderate earthquake by the viscous damper component. In case of a severe earthquake, besides the dampers, the limiter component on the weak story operates and controls the excessive deformation.

Furthermore, an energy-based damper design method was proposed to determine the necessary viscous-damper amount assuming uniform ductility distribution which can be obtained by the limiter [Sutcu F. *et al.* 2006]. Results show that the combined device compensates the low capacity of the weak-story and provides a uniform ductility distribution among the stories.

2. BUILDING MODEL AND ANALYSIS CONDITIONS

2.1 Combined energy dissipation device

Proposed energy dissipation device is combined of viscous dampers and a displacement controlling limiter device. Viscous dampers are connected to the lower beam by steel braces. The limiter was used with an adequate gap distance on the weak-story, to control the excessive displacement. The proposed device absorbs energy and decreases the structural response during a moderate earthquake by the viscous damper component. When the building is subjected to a severe earthquake, the steel brace touches the limiter on the weak story and behaves as fixed. This behavior of the steel brace prevents the excessive deformation and damage as well. However this interaction causes impact in the structure. Therefore, a rubber cushion material was used on the limiter to relief the shock in the impact. (Figure 1)

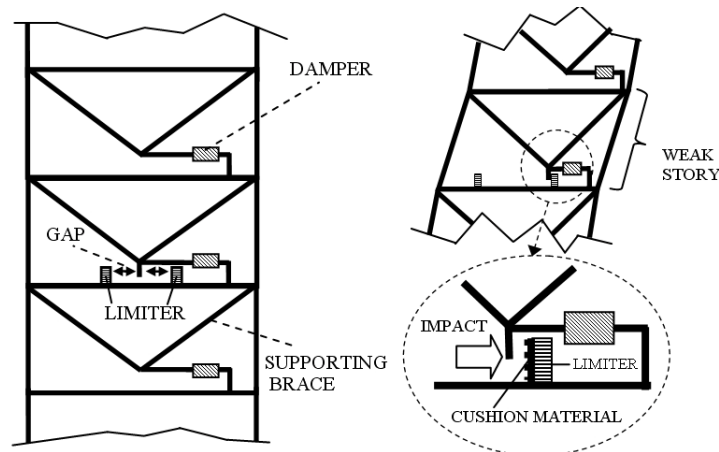


Figure 1. Combined energy dissipation device

2.2 Building model

Eleven storied reinforced concrete building model was used for the analysis. The height of each story was 3.5m. Assuming a plan with the dimensions of 18.0m x 18.0m and 1.2t/m² unit mass, the building mass was calculated 388 tons for each story. 1st natural period T_1 is given by Equation (2.1) for inelastic buildings. [IAEE 1992]

$$T_1 = 0.02 * H = 0.77 \text{sec.} \quad (2.1)$$

,where H is height (in m.) of the building. Initial stiffness of the stories was determined by initial period T_1 . Stiffness distribution through the stories was obtained by assuming initial stiffness of the top story was 1/3 that of the first story. As for inelastic force-displacement relation, degrading tri-linear model was used. It was assumed that structural damping ratio, h_s was 3% and base shear coefficient of the yielding force, $C_B=0.30$. Yield force of 6th story was assumed to be 30% less than its original value, which makes it the weak-story.

Equal amount of viscous-damper was used in each story and supported by a steel brace. Steel brace section was selected H-250x250x9x14. When two H steel members are considered as one set, the horizontal stiffness of 4 sets were computed $K_B=1560000$ kN/m and shear yielding strength was $Q_{B,y}=10892$ kN.

2.3 Analytical model

$$[M]\{\ddot{x}_{n+1}\} + [K_F]\{x_{n+1}\} + ([C_F] + [B])\{\dot{x}_{n+1}\} = -[M]\{1\}\ddot{x}_{0n+1} - \{F_{n+1}\} \quad (2.2)$$

A special analytical model was developed to calculate the behavior of the structure with proposed combined device. Final equation of motion for analytical model is shown in Equation(2.2). Here, $[M]$ is the mass matrix, $[C_F]$ is the damping matrix of the frame, $[K_F]$ is the stiffness matrix of the frame and $\{F_{n+1}\}$ is the external force term representing the resisting force of viscous-damper and limiter from the previous (n^{th}) step

2.4 Period reduction factor

In this study inelastic case parameters are evaluated from elastic properties. For such purpose the relation between elastic and inelastic cases were investigated through equivalent velocity of input energy (V_I). First, V_I spectrum was calculated for elastic case with 10% structural damping ratio. For inelastic cases, V_I spectra are calculated considering constant ductility. ($\mu=1.0, 1.5$ and 2.0) Taking the hysteretic damping into consideration, structural damping ratio for initial stiffness was assumed 5%. In Figure 2, the obvious difference between the calculated spectra is shown for 1978 Off Miyagiken earthquake, Tohoku University record.

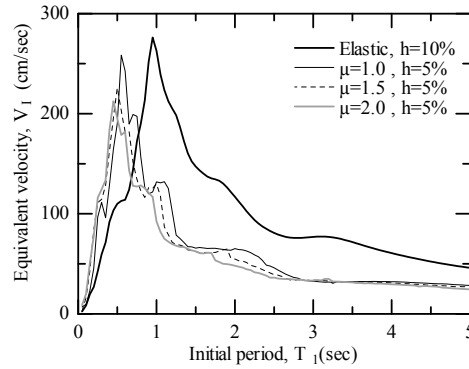


Figure 2. Comparison between elastic and inelastic equivalent velocity spectra

In the second step, obtained spectra for inelastic cases were shifted by using equivalent period (T_{eq}) in order to match each case result. Here, T_{eq} represents the equivalent period corresponding to the secant stiffness of maximum response point. (Figure 3a) Initial period T_1 may be obtained by using initial stiffness K_0 and $K_0=Q_c/\delta_c$ is known where Q_c and δ_c are crack force and displacement, respectively.

$$T_1 = 2\pi \sqrt{\frac{m\delta_c}{Q_c}} \quad (2.3)$$

T_{eq} may be obtained with a similar method.

$$T_{eq} = 2\pi \sqrt{\frac{m\delta_{max}}{Q_y}} = 2\pi \sqrt{\mu \frac{m}{K_y}}, \quad K_y = 0.3 K_0 \Rightarrow T_{eq} = \sqrt{\frac{\mu}{0.3}} T_1 \quad (2.4)$$

By Equation(2.4), T_{eq} may be defined in terms of initial period T_1 and ductility factor μ . In Figure 3b horizontal axis shows the equivalent period for inelastic cases. Therefore, inelastic spectra were shifted while elastic spectrum is constant. However this approach is not an accurate solution for linearization process as seen in the figure.

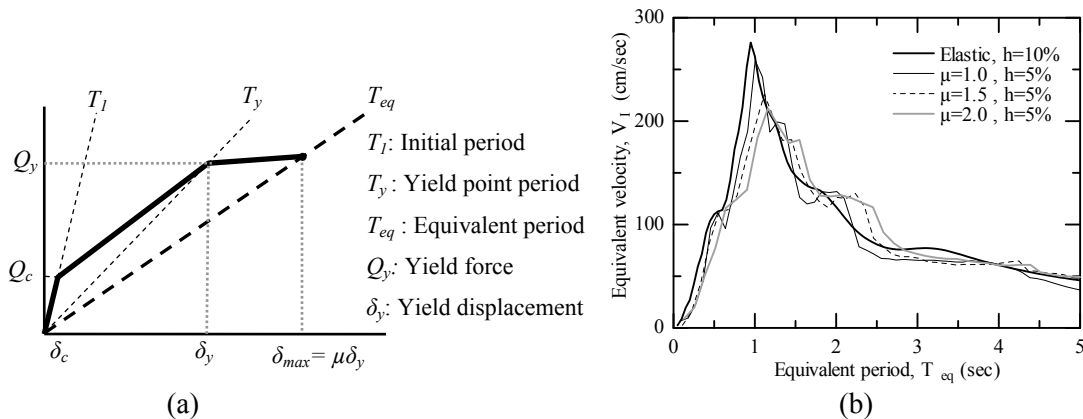


Figure 3. T_{eq} definition and equivalent period comparison between elastic equivalent velocity spectrum and inelastic equivalent velocity spectra modified by T_{eq}

Predominant period of a ground motion is generally shorter than the inelastic response period of structures except very short period range. Therefore, actual time for one hysteretic loop is considered to be shorter than T_{eq} . Finally, a “reduction factor” was proposed to obtain more accurate linearization (Figure 4a). By shifting the inelastic spectra and matching with the elastic case, Equation(2.5) was empirically proposed for reduction factor. (Figure 4b)

$$R = 1 - 0.1 \mu \quad (2.5)$$

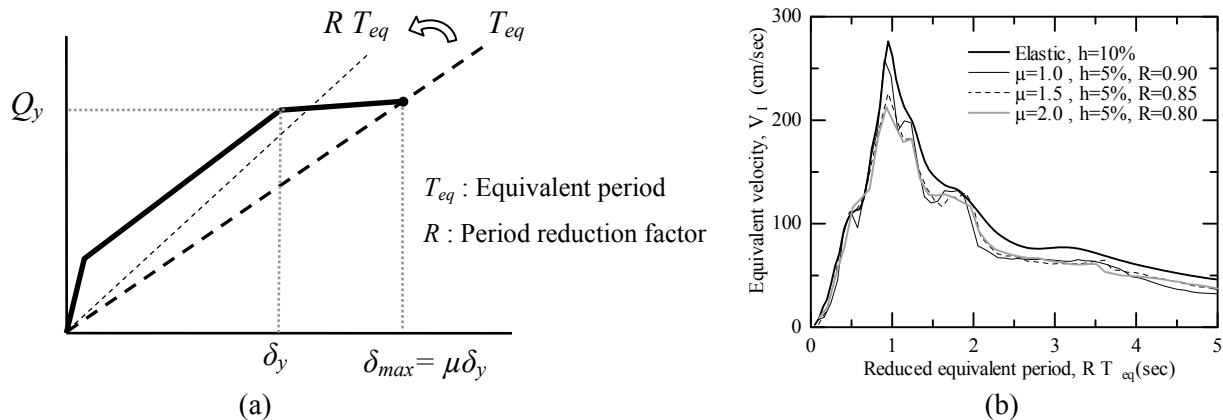


Figure 4. Period reduction factor and comparison between elastic equivalent velocity spectrum and inelastic equivalent velocity spectra modified by RT_{eq}

Reduction factor, reduced equivalent period (RT_{eq}) and natural frequency obtained by reduced equivalent period (ω_{eq}/R) were determined for different ductility factors varying from 1.0 to 2.0. Results are shown in the following table considering $T_1=0.77\text{sec}$ for the model building.

Table 1. Reduced equivalent period

μ (ductility)	T_{eq} (sec)	R	RT_{eq} (sec)	ω_{eq}/R
1.0	1.40	0.90	1.26	4.96
1.5	1.72	0.85	1.46	4.29
2.0	1.99	0.80	1.59	3.59

2.5 Input motions and normalization

Three different ground motions were used. These are the 1995 Hyogoken-Nanbu earthquake Japan Meteorological Agency (JMA) record at Kobe (N-S component), the 1978 Off Miyagiken earthquake Tohoku University record (N-S component), the 1940 El Centro earthquake (N-S component). Input motions were normalized by elastic displacement spectra (SD). For the normalization on spectra, reduced equivalent period RT_{eq} value was used. Namely, Kobe earthquake was scaled to 50cm/sec PGV (peak ground velocity). Displacement spectrum (SD) for $RT_{eq}=1.26\text{sec}$ was calculated for this scaled input motion and the rest of input motions were normalized by this spectrum. (Table 2)

Table 2. Input intensity of earthquake motions

Input Motion	Observed S_D (cm) $RT_{eq}=1.26\text{sec}$	Input intensity (%)	Input level		
			S_D (cm)	PGV (cm/sec)	PGA (gal.)
Kobe	23.79	60.5	14.4	50.0	494.8
Tohoku	15.34	93.8		39.0	193.6
El Centro	7.76	185.5		62.5	634.0

3. DAMPER DESIGN

Target of the damper design is to obtain the necessary viscous-damping coefficient (C_D) that makes maximum response ductility of the building smaller than or equal to target ductility $\mu=1.0$. For damper design, 4 steps were followed.

3.1 Step 1 - Predicted total input energy E_I

E_I was calculated by carrying out a dynamic response analysis on “equivalent linear MDOF system” where, h_S was assumed to be 10% and no additional dampers were installed. The stiffness properties of equivalent linear system were defined depending on the inelastic system. To obtain the stiffness of equivalent linear system $K_{eq.lin}$, previously defined reduced equivalent period was used.

$$K_{eq.lin} = \left(\frac{2\pi}{RT_{eq}} \right)^2 m \quad (3.1)$$

As we assume $T_{eq} = \sqrt{\frac{\mu}{0.3}} T_1$, and $T_1 = 2\pi \sqrt{\frac{m}{K_0}}$ is known, above equation becomes

$$K_{eq.lin} = \frac{0.3}{R^2 \mu} K_0 \quad (3.2)$$

Submitting $R=0.90$, $\mu=1.0$ and using matrix form for stiffness values in order to correspond MDOF system, following equation was obtained for the stiffness of equivalent linear system.

$$[K_{eq.lin}] = 0.37 [K_0] \quad (3.3)$$

3.2 Step 2 –Dissipated energy ratio

It was found out that the relation between E_I (total input energy) and E_D (total energy absorbed by damper) is depending on structural damping ratio h_S , viscous-damper damping ratio h_D and ductility factor μ . It is almost independent of initial period T_1 , input motion and input motion intensity. It is also found out that there is a good correspondence between SDOF system and MDOF systems in the means of dissipated energy ratio. To propose a relation for dissipated energy ratio, regression analysis was performed. The effective parameters, h_D , h_S and μ were used in a wide range and a generalized equation for dissipated energy ratio is proposed in Equation(3.4)

$$r = \sqrt{\frac{E_D}{E_I}} = 3.9 h_D - 2.2 h_S - 0.07 \mu + 0.757 \quad (3.4)$$

Where, r is the square root of dissipated energy ratio. Sample Variance ($V=0.0020$) and Standard Deviation ($Sx=0.0455$) were obtained as well.

3.3 Step 3 – Equivalent cycle number

As shown in Figure 5, damper response was assumed elliptical and ΔE_{Di} is the maximum energy that can be absorbed by the viscous-damper with one cycle. (Equation(3.5))

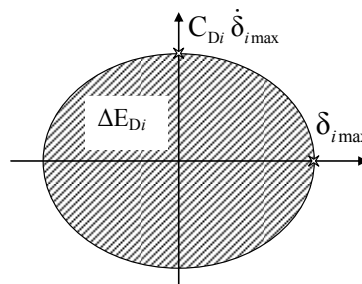


Figure 5. Assumed damper response

$$\Delta E_{Di} = \pi C_{Di} \dot{\delta}_{i\max} \delta_{i\max} \quad (3.5)$$

As E_{Di} is the total damper energy in i^{th} story, the number of equivalent cycles (n_c) that is necessary to dissipate E_{Di} can be evaluated by Equation(3.6). To evaluate n_c , SDOF was used and an equivalent cycle number spectrum was calculated for each input motion. Equivalent cycle number n_c was determined for initial period T_I and rounded down for each input motion. (Table 3)

$$n_c = \frac{E_{Di}}{\Delta E_{Di}} \quad (\text{nc: equivalent cycle number}) \quad (3.6)$$

Table 3. Assumed equivalent cycle number

Input Motion	Kobe	El centro	Tohoku
n_c equivalent cycle number	2	3	3

3.4 Step 4 - Calculation of viscous damping coefficient, C_D

By using Equation(3.5) in Equation(3.6), assuming $\dot{\delta}_{i\max} = \delta_{i\max} \omega_{eq}/R$ and $\delta_{i\max} = \mu \delta_{yi}$, and making summation among the stories, we may obtain,

$$C_D = \frac{\sum_{i=1}^{11} E_{Di}}{n_c \pi (\omega_{eq}/R) \mu^2 \sum_{i=1}^{11} \delta_{yi}^2} \quad (3.7)$$

Here in equation (3.7) it must be pointed that, “ μ^2 ” term is out of summation because, ductility was assumed to be constant as a result of limiter usage and viscous damping coefficient is changed to C_D due to the assumption that same amount of damper was used on every story. We have already obtained E_D in Step2 and $\sum E_{Di} = E_D$ is known. Finally necessary damping coefficient is obtained with the following equation.

$$C_D = \frac{E_D}{n_c \pi (\omega_{eq}/R) \mu^2 \sum_{i=1}^{11} \delta_{yi}^2} \quad (3.8)$$

3.5 Gap distance

Q_y is assumed to be constant after yielding. It was assumed that yield force of a story is the average of yield forces in one upper and one lower story and the yield force of 6th story is reduced by 30% to obtain a weak-story. As a result, some portion of the shear force on the weak-story will be supported by the limiter ($Q_{limiter}$). The non-linear hysteresis loop model for the cushion material can be used to evaluate the limiter displacement $\delta_{limiter}$ for this shear force. (Figure 6)

Brace displacement ($\delta_{brace} = Q_{limiter}/K_{brace}$) was also considered during the evaluation of the gap distance. Gap distance was obtained by Equation (3.9)

$$Gap = \mu \delta_y - (\delta_{limiter} + \delta_{brace}) \quad (3.9)$$

For this study, the gap distance was evaluated 14.0mm.

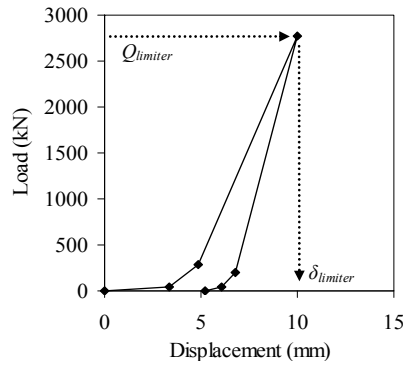


Figure 6. Evaluation of limiter displacement

4. DYNAMIC RESPONSE RESULTS

As seen on Figure 7, in the “frame only” case, especially the weak story had exceeding displacement values. It shows that, after yielding phase, severe ground motion causes excessive displacement because of the low capacity of the structure. In the “frame+damper” case, viscous-dampers with designed damping coefficients were used. By the use of viscous-dampers on each story, a significant decrease was obtained in the ductility. The average ductility seems to match the target ductility value. It was shown that, after damper design the displacement distribution among the building was smoother, significantly. Finally, in the “frame+damper+limiter” case, besides the designed dampers, the proposed displacement controlling limiter was also used on the weak story with the designed gap distribution. Therefore, exceeding displacement in the soft story was prevented and uniform displacement distribution is obtained among the building. No significant change occurred in the inertial force and acceleration values, as well. (Figure 8 and Figure 9)

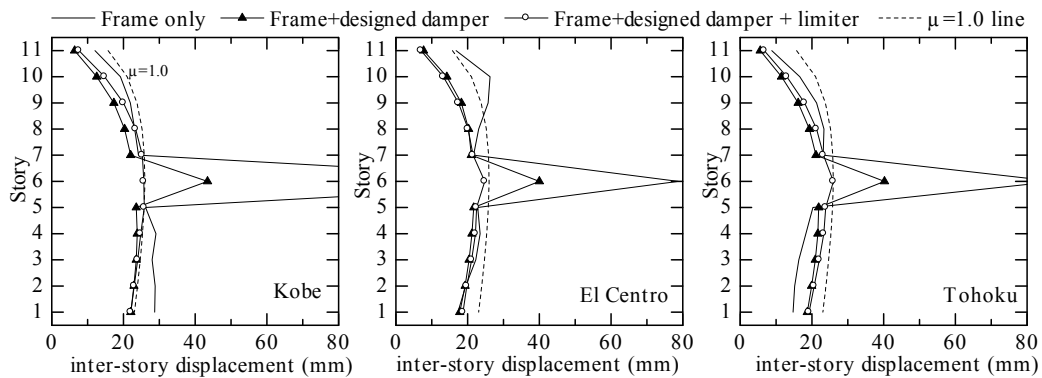


Figure 7. Maximum inter-story displacement values

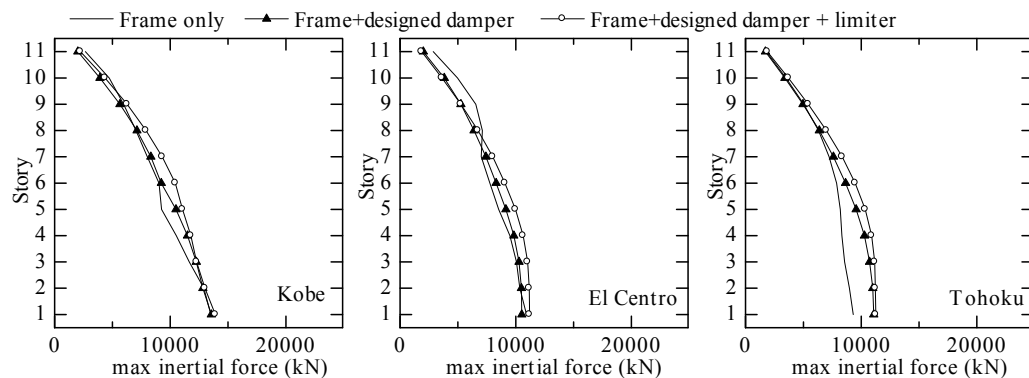


Figure 8. Maximum inertial force values

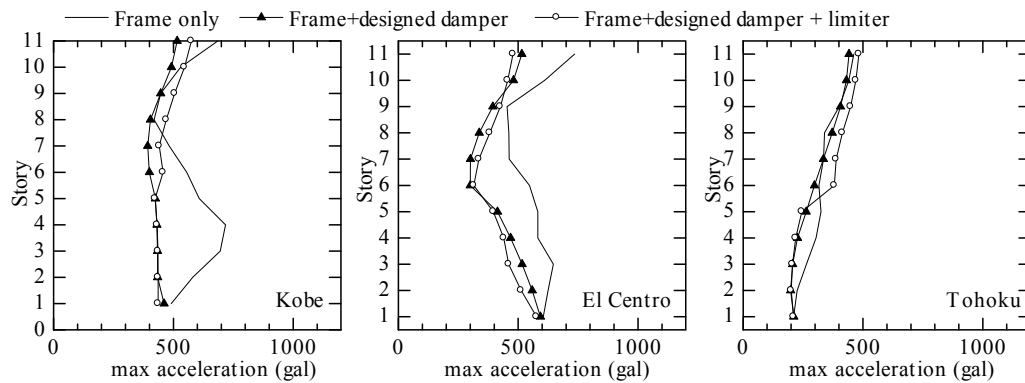


Figure 9. Maximum acceleration values

5. CONCLUSIONS

In this paper, a new design method was proposed for an energy dissipation device combined of viscous damper and displacement controlling limiter. Investigating the dynamic response results, following conclusions can be done for the study.

Exceeding displacement on the weak-story of an inelastic building can be successfully controlled by using the displacement limiter. Design of gap distance for the displacement controlling limiter was based on the lack of strength on the weak-story. After using the limiter with designed gap distance, exceeding inter-story displacement on the weak-story was reduced to the target ductility value effectively. No significant change occurred in the acceleration and inertial force values.

An energy-based damper design method was proposed to determine the necessary viscous-damping coefficient assuming uniform ductility distribution which can be obtained by the limiter. Therefore the combined device leads to an easier way for damper design as the structural response can be predicted accurately without dynamic response analysis.

These results show that proposed energy dissipation device combined of damper and displacement controlling limiter, can effectually compensate the irregularity of strength in an inelastic structure.

REFERENCES

- Hanson R.D., Kobori T. et al. (1993) State-of-the-art and state-of-the-practice in seismic energy dissipation, Proceedings of ACT-17-1 on Seismic Isolation, Energy Dissipation and Active Control; 2, 449-471.
- Kang J., Hori N., Inoue N., Kawamata S. (2004) Earthquake Resistance of Reinforced Concrete Building controlled by Device with Hardening Type Hysteresis, *13th World Conference on Earthquake Engineering*; CD-ROM, Paper No.444.
- Sutcu F., Inoue N., Hori N. (2006) Energy based damper design of a structure with a displacement controlled soft-story. *8th National Conference on Earthquake Engineering San Francisco California*; CD-ROM, Paper No.260.
- IAEE-International Association for Earthquake Engineering (1992) *Earthquake Resistant Regulations A world List*, Tokyo; 23-59.